Orbital
The electronic journal of chemistry

the electronic journal of chemistry

Full Paper | http://dx.doi.org/10.17807/orbital.v17i4.22232

Assessment of the Inhibitory Potential of Flavonoids on the Internalin A Protein of *Listeria monocytogenes* Through Molecular Docking

Cristian Sillagana-Verdezoto* [a]

Listeria monocytogenes is an intracellular pathogen capable of colonizing its hosts through virulence factors, with the Internalin A (InlA) protein being particularly notable. This study evaluated the binding affinity and interactions of 20 flavonoids through molecular docking, aiming to identify potential inhibitors of InlA. The flavonoids, selected for compliance with Lipinski's rule, were analyzed using AutoDock Vina and visualized in Chimera, PyMOL, and LigPlot+. Biological activity and pharmacokinetic predictions were conducted using PASS, ADMETlab, SwissADME, and ProTox-II, showing that the selected flavonoids have potential as antioxidant agents and membrane stabilizers. The results identified silibinin and puerarin as the compounds with the highest binding affinity (-11.93 and -10.94 kcal/mol, respectively), in addition to demonstrating potential as antioxidants and membrane stabilizers, with low toxicity. This study suggests that the selected flavonoids may inhibit the virulence of *L. monocytogenes*; however, further experimental and in vivo validation is required to confirm their inhibitory effect on InlA.

Graphical abstract

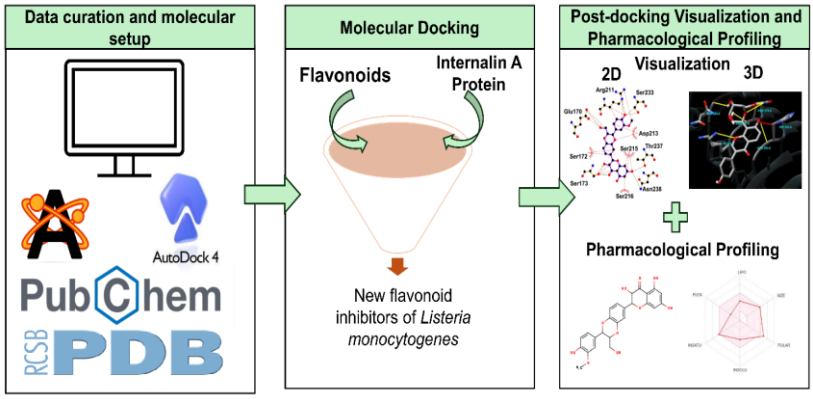

Keywords

Anti-Bacterial Agents
Flavonoids
Molecular Docking Simulation
Protein

Article history

Received 08 Nov 2024
Revised 30 May 2025
Accepted 31 May 2025
Available online 29 June 2025

Handling Editor: Adilson Beatriz

1. Introduction

Listeria monocytogenes is a facultative intracellular pathogen responsible for listeriosis, a serious disease primarily affecting immunocompromised individuals, pregnant women, neonates, and the elderly. Listeriosis is characterized by a high mortality rate, especially when it manifests as meningitis or septicemia, and has become a critical public health concern worldwide [1]. The ability of *L. monocytogenes* to cross intestinal, blood-brain, and placental barriers is facilitated by a range of virulence factors, among which the Internalin A (InlA) protein stands out [2]. This surface protein specifically interacts with E-cadherin on host cells, triggering invasion processes that are crucial for

[a] Programa de Magíster en Innovación en Biociencias y Bioingeniería, Facultad de Ingeniería, Universidad San Sebastián, Concepción, Chile. *Corresponding author. E-mail: **csillaganav@correo.uss.cl**

bacterial pathogenesis [3,4].

Inhibiting the interaction between InlA and E-cadherin represents a promising strategy to prevent *Listeria* invasion and, consequently, systemic dissemination of the infection. Advances in bioinformatics have enabled the exploration of molecular docking approaches to identify potential inhibitors [5–7]. These methods allow for rapid and efficient assessment of the binding affinity of various compounds, providing a pathway to discover new antimicrobial therapies capable of overcoming the growing resistance to conventional antibiotics [8,9].

In this context, flavonoids are promising candidates due to their broad range of biological activities, including antimicrobial, antioxidant, and anti-inflammatory properties [10–13]. Flavonoids are plant-derived secondary metabolites that share a basic structure consisting of a 15-carbon skeleton: two aromatic rings (A and B) connected by a three-carbon bridge forming a heterocyclic ring (C) [11]. This structure can be classified into different subgroups, such as flavones, flavonols, isoflavones, flavanones, catechins, and anthocyanidins, depending on the oxidation and substitution of the C ring. Functional groups on rings A and B, such as hydroxyl (-OH) groups, significantly contribute to flavonoids' ability to interact with biomolecules, affecting their affinity and specificity for binding sites [14].

The role of flavonoids in inhibiting bacterial enzymes and virulence proteins has been extensively studied. For instance, daidzein and genistein, isoflavones found in soy products, have demonstrated antimicrobial activity by modulating cellular signaling pathways in pathogens [15]. Additionally, flavonols such as kaempferol and fisetin exhibit strong potential to stabilize interactions with target proteins by forming multiple hydrogen bonds and hydrophobic interactions, enhancing their effectiveness as inhibitors of key bacterial virulence proteins [16]. Furthermore, compounds like quercetin and rutin have shown synergistic activities when combined with antibiotics [17,18].

Given that InlA plays a fundamental role in the invasion and pathogenesis of *Listeria monocytogenes*, this study focuses on evaluating the binding affinity and potential interactions of a selected set of flavonoids through molecular docking to identify potential inhibitors capable of interfering with the InlA-E-cadherin interaction.

2. Results and Discussion

Most of the 20 flavonoids complied with Lipinski's rule of five, which requires a molecular weight below 500 g/mol, no more than 5 hydrogen bond donors, 10 hydrogen bond acceptors, and a logP partition coefficient of 5 or less [19]. Daidzein and chrysin had the lowest molecular weights (~254 g/mol), while puerarin and silybin were the heaviest and showed the highest numbers of hydrogen bond donors and acceptors. Notably, puerarin exceeded the donor limit with 6 hydrogen bond donors. **Table 1** highlights the overall potential of these flavonoids for oral administration, as the majority meet the criteria used to predict drug-likeness in humans [20].

Table 1. Selected flavonoids that comply with Lipinski's rule for molecular docking with the InlA protein.

Flavonoid	Molecular Weight (g/mol)	H-bond Donors	H-bond Acceptors	LogP
Daidzein	254.06	2	4	2.79
Chrysin	254.06	2	4	3.58
Apigenin	270.05	3	5	3.30
Genistein	270.05	3	5	2.50
Galangin	270.05	3	5	3.26
Baicalein	270.05	3	5	3.21
Naringenin	272.07	3	5	2.59
Fisetin	286.04	4	6	1.8
Kaempferol	286.05	3	8	3.99
Luteolin	286.05	4	6	2.90
Eriodictyol	288.06	4	6	2.14
(-)-Catechin	290.08	5	6	1.16
(-)-Epicatechin	290.08	5	6	1.21
Quercetin	302.04	5	7	1.82
Morin	302.04	5	7	2.07
Hesperetin	302.08	3	6	2.49
Taxifolin	304.06	5	7	0.44
Isorhamnetin	316.06	4	7	2.54
Puerarin	416.11	6	9	0.69
Silybin	482.12	5	10	2.21

Blind molecular docking was performed between the InlA protein and the 20 ligands selected in **Table 1**. **Fig. 1** and **Table 2** show the five ligands with the highest binding affinity to the InlA protein of *L. monocytogenes*. Silybin presented the highest affinity with a binding affinity energy of -11.92 kcal/mol. Previous studies indicate that more negative binding affinity values reflect greater interaction efficiency between the ligand and the protein [23–25]. The ligands fisetin, genistein and daidzein were able to bind to the Phe150 residue of InlA, which is involved in binding to human E-cadherin at its Pro16 residue in a cis conformation [3]. These five ligands demonstrated high binding affinity values to InlA, suggesting a potential capacity to inhibit the function of this protein.

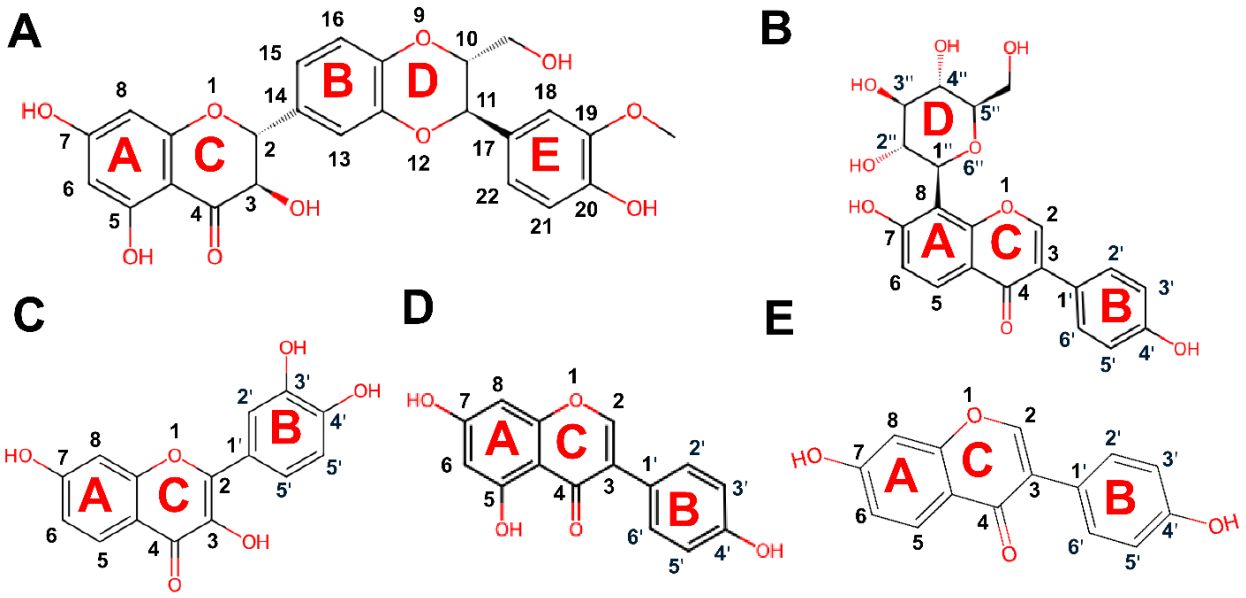

Fig. 1. Chemical structure of the five flavonoids with the best docking results with the InlA protein. A) Silybin B) Puerarin C) Fisetin D) Genistein E) Daidzein.

Table 2. Molecular docking results of the five ligands (flavonoids) with the best docking scores with the InlA protein.

Ligand name	Binding affinity (kcal/mol)	Amino acid residues involved (Pymol, 3D)		Amino acid residues involved (LigPlot+, 2D)	
		H-bond	Hydrophobic	H-bond	Hydrophobic
Silybin	-11.93	Ser 173, Ser 233, Thr 237, Asn 238		Glu 170, Ser173, Arg 211, Ser 233, Thr 237, Asn 238	Ser 172, Asp 213, Ser 215, Ser 216
Puerarin	-10.94	Asn 350, Asn 370, Lys 372, His 392	His392	Asn 349, Asn 370	Asn 350, Asn 371, His 392, Gln 394, Ala 416, Trp 417, Thr 418
Fisetin	-10.84	Glu 170		Leu 191	Phe 150, Ser 172, Ser 192, Arg 211, Leu 212, Asp 213
Genistein	-10.08	Ser 192, Ser 233		Ser 192, Arg 211	Phe 150, Asp213, Ser 233
Daidzein	-9.66	Ser 192, Ser 233		Ser 192, Arg 211, Ser 233	Phe 150, Asp 213

The ligands silybin and puerarin were the flavonoids with the most binding interactions when docked with InlA (**Table 1**). In the Chimera visualization, silybin showed three hydrogen bonds (**Table 1**, **Figure 2A**), while in LigPlot+ it displayed six hydrogen bonds and four hydrophobic interactions (**Table 1, Figure 3A**). Puerarin, in turn, exhibited four hydrogen bonds and one hydrophobic interaction in Chimera (**Table 1**, **Figure 2B**), and two hydrogen bonds and seven hydrophobic interactions in LigPlot+ (**Table 1**, **Figure 3B**). In a recent study by Deepasree and Subharshree (2024) [23], bipinnatin, a terpene that showed better docking with InlA, presented a binding affinity of -9.5 kcal/mol, with two hydrophobic interactions and one hydrogen bond in the 3D visualization, and three hydrogen bonds and three hydrophobic interactions in LigPlot+. Unlike terpenes, the flavonoids in our study presented better binding characteristics when docked with the InlA protein.

This may be due to their ability to form stable interactions within or near the E-cadherin binding interface of InlA. Although the main interacting residues observed (e.g., Ser173, Asn238, Thr237), are not part of the core E-cadherin contact residues (Tyr343, Phe367, Tyr387, Phe150, Tyr347), they are located within the general interface region and may influence protein surface accessibility or flexibility. The multiple hydroxyl and ether groups present in the flavonoid scaffold enable the formation of dense hydrogen bond networks, which may stabilize the ligand–protein complex and reduce conformational freedom of InlA. This structural stabilization, especially near the entry site of the E-cadherin-binding groove, could lead to steric hindrance or allosteric modulation that interferes with host-cell adhesion, ultimately contributing to reduced virulence.

In silybin, the C-ring forms two hydrogen bonds: one through the carbonyl group and the other with the hydroxyl group, both interacting with the Ser173 residue. The hydroxyl group at position 7 on ring A establishes hydrogen bonds with the Asn238 and Thr237 residues, while on ring E, the hydroxyl group forms a hydrogen bond with Ser233 (**Figure 2A**). In puerarin, the hydroxyl group on ring A establishes a hydrogen bond with His392, and the ether group on ring C forms a hydrogen bond with Lys372. In ring D, which contains a glucose ring attached to the isoflavonoid core via a glycosidic bond, the ether group and the hydroxyl group at carbon position 4 interact through hydrogen bonds with Asn370. The hydroxyl group at carbon position 2 interacts with His393 via a hydrogen bond and forms a hydrophobic interaction with Asn393; additionally, the hydroxyl group attached to carbon 6 forms a hydrogen bond with Asn370 (**Figure 2B**). These results suggest that the glycosylated moiety of puerarin plays a key role in enhancing polar interactions with InlA, contributing to its high binding affinity despite exceeding the hydrogen bond donor limit set by Lipinski's rule.

Fisetin presents two hydrogen bonds between the hydroxyl group on ring C and Glu170 (**Figure 2C**). Genistein forms a hydrogen bond through the hydroxyl group at position 7 on ring A with Ser233 and establishes two additional bonds: one through the hydroxyl group at position 5 on ring A and another via the carbonyl group on ring C with Ser192 (**Figure 2D**). Daidzein presents a hydrogen bond between the hydroxyl group on ring A and Ser233, and another between the carbonyl group on ring C and Glu170 (**Figure 2E**).

Our results show a high affinity of the ligands to form hydrogen bonds when docked with the InlA protein. Pace et al. demonstrated that hydrogen bond formation by -OH groups significantly contribute to protein stability [26]. Additionally, polar groups that do not form hydrogen bonds with the protein can also favor its stability [27]. These functional groups include hydroxyls, carbonyls, carboxyls, ethers, and amino acids distributed across the flavonoid skeletons.

As a means of methodological validation, a redocking repetition protocol was implemented to verify the internal consistency of the docking results. This strategy serves as an *in silico* control to confirm the reproducibility of the binding affinities obtained with AutoDock Vina, reinforcing the reliability of the predicted ligand–protein interactions. Similar validation strategies have been employed in large-scale molecular docking analyses to increase the robustness of virtual screening results. For example, Sorzano et al. (2020) performed multitarget docking campaigns for drug repurposing in COVID-19 and emphasized the importance of internal consistency and methodological control during prediction stages [28].

Table 3 summarizes the binding affinities obtained in these five runs, along with the calculated average and standard deviation for each ligand. The low variability (standard deviation< 0.026 kcal/mol) confirms that the docking protocol used produces stable and reproducible results under repeated conditions.

Table 3. Binding Affinity Values from Five Independent Docking Runs for the Top Five Flavonoids

Ligand name	Run1 (kcal/mol)	Run 2 (kcal/mol)	Run 3 (kcal/mol)	Run 4 (kcal/mol)	Run 5 (kcal/mol)	Average (kcal/mol)	Standard deviation (kcal/mol)
Silybin	-11.920	-11.928	-11.932	-11.938	-11.935	-11.9306	0.006
Puerarin	-10.900	-10.932	-10.972	-10.968	-10.959	-10.9462	0.026
Fisetin	-10.850	-10.808	-10.859	-10.856	-10.845	-10.8436	0.018
Genistein	-10.080	-10.082	-10.083	-10.09	-10.092	-10.0854	0.004
Daidzein	-9.670	-9.662	-9.669	-9.658	-9.677	-9.6672	0.006

Once in the body, the mechanism of action of a biologically active compound is determined by its absorption, distribution, metabolism, excretion, and toxicity (ADMET). Evaluating and optimizing the action and efficacy of a bioactive compound requires knowledge of its pharmacokinetic profile [20]. These findings suggest that although silybin and puerarin displayed the strongest binding affinities to InlA *in silico* (**Table 4**), their predicted pharmacokinetic profiles may limit their oral bioavailability due to low gastrointestinal absorption and low Caco-2 permeability. This could reduce their systemic exposure unless alternative delivery methods (e.g., nanoformulations or intravenous routes) are considered. In contrast, fisetin, genistein, and daidzein combine favorable binding energies with higher predicted absorption and permeability, making them more attractive candidates for systemic therapeutic use. All compounds fell within toxicity classes 3–5, indicating acceptable safety margins. Moreover, their synthetic accessibility scores suggest that they can be feasibly synthesized for further experimental validation.

Table 5 shows the predicted biological activities of the five ligands according to PASS Online. Most flavonoids exhibited high Pa values as membrane integrity agonists and membrane permeability inhibitors. These properties may be beneficial in protecting host cells and reducing bacterial adhesion or invasion, which aligns with the proposed mechanism of InlA–E-cadherin interaction. Although direct antimicrobial activity was not predicted for any of the compounds, this does not exclude potential virulence inhibition via host cell stabilization or interference with bacterial internalization processes.

Additionally, several ligands showed high probabilities for antioxidant-related activities, such as free radical scavenging and antimutagenic effects, which are consistent with the known pharmacological profile of flavonoids. These properties could further contribute to tissue protection during infection. The activity predictions provide complementary evidence supporting the potential of these flavonoids as multifunctional agents with possible indirect anti-*Listeria* effects.

Table 4. Pharmacological properties of the five ligands (flavonoids) with the InlA protein.

Compound	Gastrointestinal absorption[a]	BBB permeant[b]	Caco-2 permeability[c]	Toxicity class[d]	Synthetic accessibility[e]
Silybin	Low	No	-6.295	4	4.92
Puerarin	Low	No	-6.199	4	4.98
Fisetin	High	No	-4.987	3	3.16
Genistein	High	No	-4.764	5	2.87
Daidzein	High	Yes	-4.643	5	2.79

[a]Gastrointestinal absorption: Qualitative prediction of oral absorption (High/Low) based on molecular descriptors, from SwissADME [29]. [b]BBB permeant: Indicates the predicted ability to cross the blood–brain barrier (Yes/No), based on polarity and size filters [29]. [c]Caco-2 permeability: Predicted logPapp (log apparent permeability) across Caco-2 cells; values below -5.15 suggest poor permeability [30]. [d]Toxicity class: Toxicological classification based on LD_{50} values from ProTox-II, ranging from class 1 (most toxic) to class 6 (least toxic) [31]. [e]Synthetic accessibility: Score from 1 (very easy to synthesize) to 10 (very difficult), based on fragment contributions and molecular complexity [29].

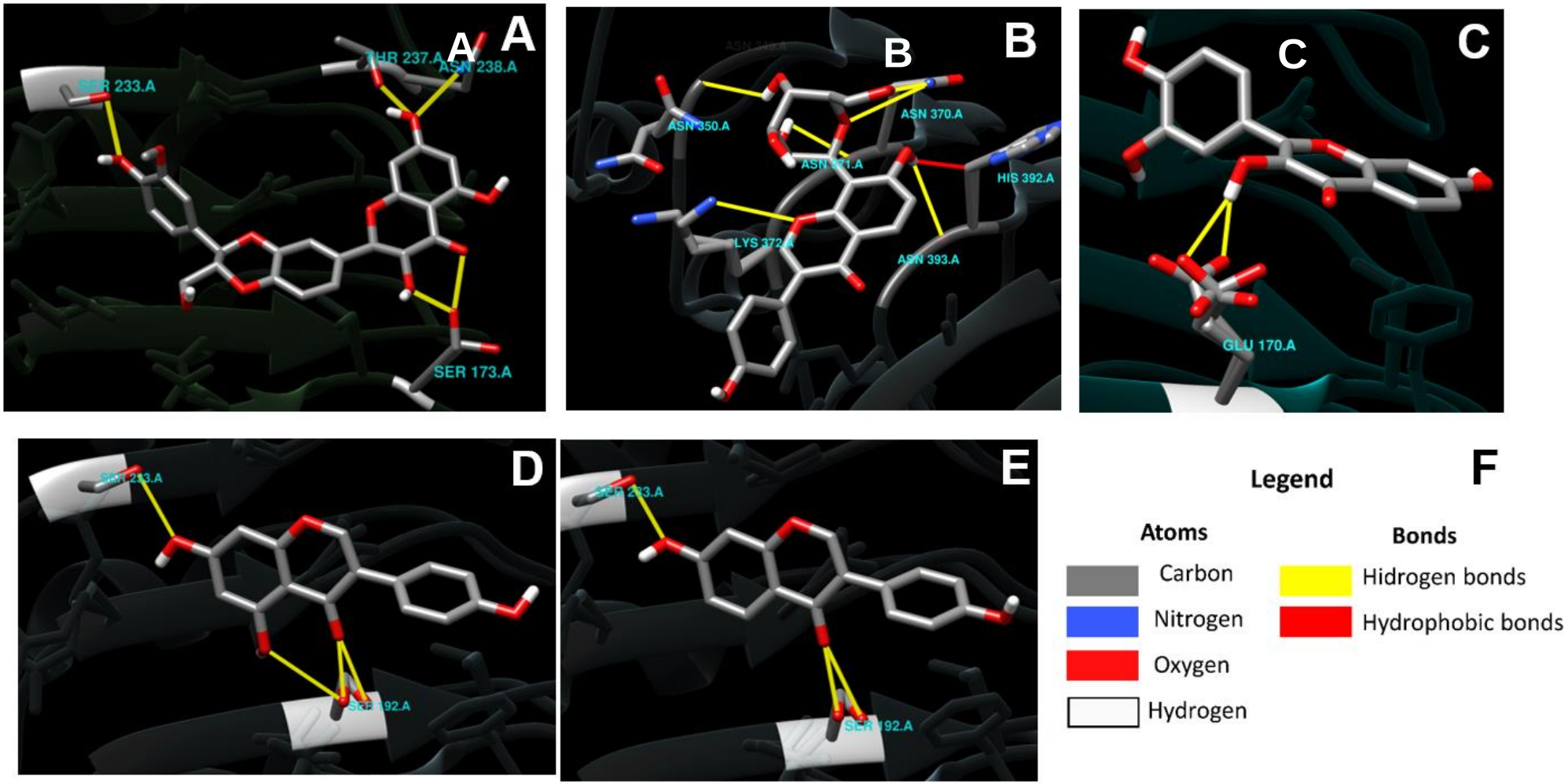

Fig. 2. Molecular docking details of the five ligands (flavonoids) with the InlA protein visualized in 3D structure. Colors represent chemical structure: yellow lines for hydrogen bonds, red lines for hydrophobic interactions, gray for carbon, red for oxygen, blue for nitrogen, yellow for sulfur. A) Silybin B) Puerarin C) Fisetin D) Genistein E) Daidzein F) .

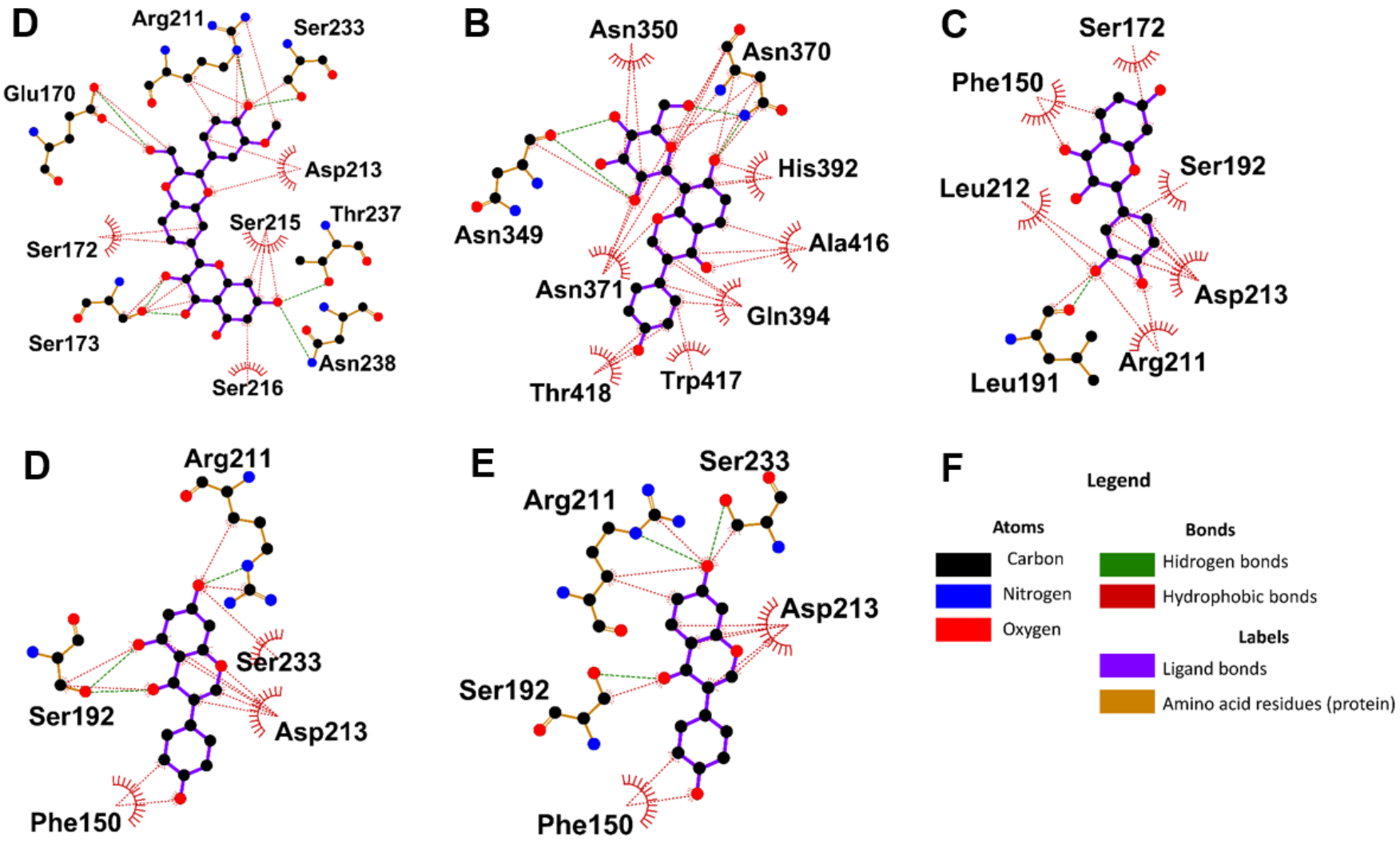

Fig. 3. Molecular docking details of the five ligands (flavonoids) with the InlA protein visualized in 2D structure. A) Silybin B) Puerarin C) Fisetin D) Genistein E) Daidzei F) Legend.

Table 5. Predicted biological activities of the five ligands (flavonoids) with the InlA protein.

Compound	Biological activity	Pa (Probability to be Active)[a]	Pi (Probability to be Inactive)[a]
Silybin	Free radical scavenger	0.956	0.001
	Membrane integrity agonist	0.957	0.003
	Hepatoprotectant	0.939	0.002
	APOA1 expression enhancer	0.936	0.002
	TP53 expression enhancer	0.914	0.005
Puerarin	Cardioprotectant	0.937	0.002
	Hepatoprotectant	0.906	0.002
	Cytostatic	0.876	0.004
	Anticarcinogenic	0.851	0.004
	Chemopreventive	0.823	0.004
Fisetin	Chlordecone reductase inhibitor	0.978	0.001
	Membrane integrity agonist	0.966	0.002
	Aryl-alcohol dehydrogenase (NADP+) inhibitor	0.959	0.001
	Membrane permeability inhibitor	0.954	0.002
	Antimutagenic	0.943	0.001
Genistein	Membrane integrity agonist	0.913	0.008
	Membrane permeability inhibitor	0.888	0.004
	Antimutagenic	0.874	0.003
	Antiseborrheic	0.832	0.013
	Vasoprotector	0.822	0.004
Daidzein	Membrane integrity agonist	0.887	0.014
	Membrane permeability inhibitor	0.850	0.005
	Antimutagenic	0.836	0.003
	Antiseborrheic	0.835	0.013
	Peroxidase inhibitor	0.797	0.005

[a]Values correspond to the predicted probability of activity (Pa) calculated by the PASS tool. According to Lagunin *et al*. (2000), compounds with Pa > 0.7 are very likely to exhibit the predicted activity experimentally, while values between 0.5 and 0.7 suggest moderate likelihood, and values below 0.5 indicate low probability of activity [32].

Molecular docking performed with AutoDock Vina enabled the identification of key protein-ligand interactions. This approach could benefit in the future from complementary tools, such as molecular dynamics simulations, which would provide a broader perspective on the stability of complexes under conditions closer to the biological environment, thereby enriching the interpretation of the results without compromising the robustness of the findings obtained in this study

3. Material and Methods

3.1. Preparation of the Protein and Ligands

The three-dimensional structure of the *Listeria monocytogenes* protein Internalin A (InlA) was obtained from the Protein Data Bank (PDB) with a resolution of 1.50 Å (PDB ID: 1O6V) [33]. Protein preparation was conducted using AutoDock Tools version 1.5.7. During this process, water molecules and heteroatoms were removed, polar hydrogens were added, and Kollman charges were assigned. The prepared receptor structure was saved in PDBQT format for docking simulations.

For the ligands, twenty flavonoids with reported antimicrobial activity were selected based on compliance with Lipinski's rule of five (**Table 1**). Molecular properties (molecular weight, hydrogen bond donors/acceptors, and logP) were obtained from the NPASS database [34]. Their 2D structures were retrieved in SDF format from the PubChem database. Each molecule was converted into 3D using Avogadro version 1.2.0 [35] and energy-minimized using the steepest descent algorithm with 500 steps. The optimized molecules were saved in MOL2 format. Ligand protonation and torsion flexibility were assigned in AutoDock Tools, and the final files were converted into PDBQT format for docking.

3.2. Molecular Docking between InlA and Flavonoids

Molecular docking was performed using AutoDock Vina version 1.2. [36] to evaluate the interaction between 20 flavonoids and the InlA protein, aiming to identify molecular interactions involved in the binding process. AutoDock Vina employs a combined scoring function and a gradient-based search algorithm to predict binding modes [37,38]. During docking, the protein was kept rigid, while the ligands were flexible, allowing rotatable bonds to adopt favorable conformations.

The docking grid was centered at coordinates x = 5.017, y = 6.016, z = 149.855, with dimensions of 58 × 58 × 52 Å, and a grid spacing of 1 Å. These parameters ensured that the residues Tyr343, Phe367, Tyr387, Phe150, and Tyr347, known to be involved in interactions with E-cadherin, were included within the search space (**Supplementary Material 1)**.

The exhaustiveness parameter was set to 8, balancing computational cost and search depth. Docking was executed through a batch script via the command line in Windows, automating the process for all 20 ligands (**Supplementary Material 2**). The five flavonoids with the best binding affinities (lowest ΔG values) were selected for further protein–ligand interaction analysis.

3.3. Method Validation by Redocking

Method validation was carried out by performing five independent docking runs for each of the five flavonoids with the best binding affinities from the initial screening. All

docking parameters, including grid dimensions and search conditions, were kept constant across all repetitions. The same ligand and receptor files were used in each run.

3.4. Visualization of Binding Interactions

Protein-ligand interactions and the involved residues were analyzed using PyMOL and Chimera 1.18 [39] for 3D visualization, and LigPlot+ [40] for 2D visualization. Interactions, such as hydrogen bonds and hydrophobic interactions, were examined in detail. For LigPlot+ visualization, the atomic coordinates section of the ligand was copied from the PDBQT file and pasted into the protein file in PDB format, placing it after the amino acid chain and before the END line. The combined file was verified in Chimera 1.18 before being used in LigPlot+.

3.5. Prediction of Biological Activities and Pharmacokinetic Properties

The five selected flavonoids were downloaded in molfile format from the ChEBI database and converted to SMILES format. Biological activities were predicted using PASS (Prediction of Activity Spectra for Substances) [32]. Pharmacokinetic properties, such as absorption, distribution, metabolism, excretion, and toxicity (ADMET), were analyzed with ADMETlab [30] and SwissADME [29]. Toxicity levels were evaluated using ProTox-II [31].

4. Conclusions

This study evaluated the potential of 20 flavonoids to inhibit the virulence protein Internalin A (InlA) of *Listeria monocytogenes*. Among them, silybin and puerarin showed the highest binding affinity (-11.92 and -10.90 kcal/mol, respectively) compared to ampicillin, suggesting they could be promising candidates for targeting InlA. Additionally, these compounds displayed favorable biological activity profiles, low toxicity, and ease of synthesis. Therefore, the *in silico* results indicate that silybin, puerarin, fisetin, genistein, and daidzein could interfere with the interaction between InlA and E-cadherin, thereby reducing the virulence potential of *L. monocytogenes*. Future studies are recommended to validate their inhibitory potential through *in vitro* and *in vivo* assays for the development of drugs targeting this virulence protein.

Supporting Information

Supplementary Material 1 and 2.

Author Contributions

The author was solely responsible for conceptualizing the study, conducting all experiments, analyzing the data, and preparing the manuscript.

References and Notes

[1] Schlech, W. F. *Microbiol Spectr*. **2019**, 7. [Crossref]

[2] Lecuit, M. *Clin. Microbiol. Infect.* **2005**, *11*, 430. [Crossref]

[3] Schubert, W. D.; Urbanke, C.; Ziehm, T.; Beier, V.; Machner, M. P.; Domann, E.; Wehland, J.; Chakraborty, T.; Heinz, D. W. *Cell* **2002**, *111*, 825. [Crossref]

[4] Gaillard, J. L.; Berche, P.; Frehel, C.; Gouln, E.; Cossart, P. *Cell* **1991**, *65*, 1127. [Crossref]

[5] Agu, P. C.; Afiukwa, C. A.; Orji, O. U.; Ezeh, E. M.; Ofoke, I. H.; Ogbu, C. O.; Ugwuja, E. I.; Aja, P. M. *Sci. Rep.* **2023**, 13. [Crossref]

[6] Mohammad, T.; Hussain, A.; Alajmi, M. F.; Hasan, S.; Yadav, D. K.; Hassan, M. I. *Chem. Phys. Impact* **2024**, *8*, 100458. [Crossref]

[7] Vardhan, S.; Sahoo, S. K. *Comput. Biol. Med*. **2020**, 124103936. [Crossref]

[8] Anza, M.; Endale, M.; Cardona, L.; Cortes, D.; Eswaramoorthy, R.; Zueco, J.; Rico, H.; Trelis, M.; Abarca, B. *Adv. Appl. Bioinf. Chem*. **2021**, *14*, 117. [Crossref]

[9] Marinho, A. M. R.; de Oliveira, C. M. S. C.; Silva-Silva, J. V.; de Jesus, S. C. A.; Siqueira, J. E. S.; de Oliveira, L. C.; Auzier, J. F.; Soares, L. N.; Pinheiro, M. L. B.; Silva, S. C. *et al*. *Antibiotics* **2023**, 12, 1331. [Crossref]

[10] Ullah, A.; Munir, S.; Badshah, S.L.; Khan, N.; Ghani, L.; Poulson, B. G.; Emwas, A. H.; Jaremko, M. *Molecules* **2020**, *25*, 5243. [Crossref]

[11] Dias, M. C.; Pinto, D. C. G. A.; Silva, A. M. S. *Molecules* **2021**, *26*, 5377. [Crossref]

[12] Yin, L.; Han, H.; Zheng, X.; Wang, G.; Li, Y.; Wang, W. *Ind. Crops Prod*. **2019**, *137*, 652. [Crossref]

[13] Hasnat, H.; Shompa, S. A.; Islam, M. M.; Alam, S.; Richi, F. T.; Emon, N. U.; Ashrafi, S.; Ahmed, N. U.; Chowdhury, M. N. R.; Fatema, N. *et al*. *Heliyon* **2024**, *10*, e27533. [Crossref]

[14] Panche, A. N.; Diwan, A. D.; Chandra, S. R. *J. Nutr. Sci*. **2016**, *5*, e47. [Crossref]

[15] Wang, T.; Liu, Y.; Li, X.; Xu, Q.; Feng, Y.; Yang, S. *J. Sci. Food Agric.* **2018**, *98*, 2043. [Crossref]

[16] Kumar, S.; Pandey, A. K. *Sci. World J.* **2013**, *2013*, 162750. [Crossref]

[17] Deepika, M. S.; Thangam, R.; Vijayakumar, T. S.; Sasirekha, R.; Vimala, R. T. V.; Sivasubramanian, S.; Arun, S.; Babu, M. D.; Thirumurugan, R. *Microb. Pathog.* **2019**, *135*, 103612. [Crossref]

[18] Alnour, T. M. S.; Ahmed-Abakur, E. H.; Elssaig, E. H.; Abuduhier, F. M.; Ullah, M. F. *Ital. J. Food Sci.* **2022**, *34*, 34. [Crossref]

[19] Benet, L. Z.; Hosey, C. M.; Ursu, O.; Oprea, T. I. *Adv. Drug Deliv. Rev*. **2016**, *101*, 89. [Crossref]

[20] Lipinski, C. A.; Lombardo, F.; Dominy, B. W.; Feeney, P. J. *Adv. Drug Deliv. Rev.* **2012**, *64*, 4. [Crossref]

[21] Rodríguez-Auad, J. P. *Revista Chilena de Infectología* **2018**, *35*, 649. [Crossref]

[22] Grosboillot, V.; Keller, I.; Ernst, C.; Loessner, M. J.; Schuppler, M. *Front Cell Infect. Microbiol*. **2022**, *12*, 869339. [Crossref]

[23] Deepasree, K.; Venugopal, S. *Frontiers in Bioinformatics* **2024**, *4*, 1463750. [Crossref]

[24] Deepasree, K.; Subhashree, V. *Inform. Med.Unlocked*. **2023**, *39*, 101252. [Crossref]

[25] Jian, Y.; Wu, C.; Reidenbach, D.; Krishnapriyan, A. S. arXiv:2406.16821 2024. [Crossref]

[26] Pace, C. N.; Fu, H.; Fryar, K. L.; Landua, J.; Trevino, S. R.; Schell, D.; Thurlkill, R. L.; Imura, S.; Scholtz, J. M.; Gajiwala, K. *et al*. *Protein Science* **2014**, *23*, 652. [Crossref]

[27] Schell, D.; Tsai, J.; Scholtz, J. M.; Pace, C. N. *Function and Genetics* **2006**, *63*, 278. [Crossref]

[28] Sorzano, C.; Crisman, E.; Carazo J.; Leon, R. *ChemRxiv* **2020**. [Crossref]

[29] Diana, A.; Michielin, O.; Zoete, V. *Sci. Rep.* **2017**, *7*, 42717. [Crossref]

[30] Xiong, G.; Wu, Z.; Yi, J.; Yang, Z.; Hsieh, C.; Yin, M.; Zeng, X.; Wu, C.; Lu, A.; Chen, X.; Hou, T.; Cao, D. *Nucleic Acid Res.* **2021**, *W5*, 49. [Crossref]

[31] Banerjee, P.; Eckert, A.; Schrey, A.; Preissner, R. *Nucleic Acid Res*. **2018**, *W1*, 46. [Crossref]

[32] Lagunin, A.; Stepachikova, A.; Filimonov, D.; Poroikov, V. *Bioinformatics* **2000**, *8*, 16. [Crossref]

[33] Schubert, W.-D.; Urbanke, C.; Ziehm, T.; Beier, V.; Machner, M. P.; Domann, E.; Wehland, J.; Chakraborty, T.; Heinz, D. W. *Cell* **2002**, *111*, 825. [Crossref]

[34] Zeng, X.; Zhang, P.; He, W.; Qin, C.; Chen, S.; Tao, L.; Wang, Y.; Tan, Y.; Gao, D.; Wang, B.; Chen, Z.; Chen, W.; Yang, Y.; Zong, Y. *Nucleic Acid Res.* **2018**, *46*, D1. [Crosssref]

[35] Hanwell, M.; Curtis, D.; Lonie, D.; Vandermeersch, T.; Zurek, E.; Hutchison, G. *J. Cheminform*. **2012**, *4*, 17. [Crossref]

[36] Trott, O.; Olson, A. *J. Comput Chem*. **2010**, *2*, 31. [Crossref]

[37] Eberhardt, J.; Santos-Martins, D.; Tillack, A. F.; Forli, S. *J. Chem. Inf. Model*. **2021**, *61*, 3891. [Crossref]

[38] Trott, O.; Olson, A. J. *J. Comput. Chem*. **2010**, *31*, 455. [Crossref]

[39] Pettersen, E. F.; Goddard, T. D.; Huang, C. C.; Couch, G. S.; Greenblatt, D. M.; Meng, E. C.; Ferrin, T. E. *J. Comput. Chem*. **2004**, *25*, 1605. [Crossref]

[40] Laskowski, R. A.; Swindells, M. B. *J. Chem. Inf. Model*. **2011**, *51*, 2778. [Crossref]

How to cite this article

Sillagana-Verdezoto, C. *Orbital: Electronic J. Chem*. **2025**, *17*, 297. DOI: http://dx.doi.org/10.17807/orbital.v17i4.22232